Pressure-induced removal of magnetostructural inhomogeneity in Ge-rich $Gd_5(Si_xGe_{1-x})_4$ giant magnetocaloric alloys

Y. C Tseng,[1,2] D. Haskel,[2,*] N. M. Souza-Neto,[2] Ya. Mudryk,[3] V. K. Pecharsky,[3,4] and K. A. Gschneidner, Jr.[3,4]
[1]*Department of Materials Science and Engineering, Northwestern University, Evanston, Illinois 60201, USA*
[2]*Magnetic Materials Group, Advanced Photon Source, Argonne National Laboratory, Argonne, Illinois 60439, USA*
[3]*Ames Laboratory, Iowa State University, Ames, Iowa 50011-3020, USA*
[4]*Department of Materials and Engineering, Iowa State University, Ames, Iowa 50011-2300, USA*
(Received 24 October 2008; published 30 December 2008)

We investigate the emergence of ferromagnetism (FM) in low-Si-content $Gd_5(Si_xGe_{1-x})_4$ alloys ($x=0.025, 0.05, 0.075$) from within the antiferromagnetic (AFM) phase of the Gd_5Ge_4 parent compound. X-ray magnetic circular dichroism (XMCD) and bulk magnetization measurements show that all samples exhibit partial FM order at low temperature, but their saturation magnetization is reduced relative to higher-Si-content samples ($x=0.125, 0.5$). This reduced magnetization is due to an incomplete AFM orthorhombic(II) $\rightarrow$FM orthorhombic(I) magnetostructural phase transition upon cooling, as evidenced by x-ray diffraction. High-pressure XMCD measurements in a diamond-anvil cell show that applied pressures of 5.0, 3.0, and 2.0 GPa restore the full saturation magnetization in $x=0.025$, 0.05, and 0.075 samples, respectively, by stabilizing the FM-O(I) phase. The mixed-phase behavior is also evidenced in dT_c/dP, which strongly varies with silicon concentration in these samples at low pressures but becomes independent of x at higher pressures where values typical of higher-x samples ($0.125<x<0.5$) are found.

DOI: 10.1103/PhysRevB.78.214433 PACS number(s): 71.20.Eh, 75.30.Sg, 75.25.+z

I. INTRODUCTION

$Gd_5(Si_xGe_{1-x})_4$ alloys have generated significant attention because of their potential use as refrigerants in magnetic cooling devices.[1–3] Their sizable magnetocaloric effect is due to a first-order magnetostructural transition,[4–7] which can be reversibly induced by an applied magnetic field. The sudden change in magnetic and structural entropies in the vicinity of this magnetostructural transition can be harnessed for magnetic refrigeration applications. For example, adiabatic temperature changes as large as 16 K have been observed for $x\sim0.5$ near its transition temperature of $\sim$275 K in applied fields below 5 T.[6]

While the ferromagnetic nature of these compounds for $x\gtrsim0.2$ is now well established, the low-x region of the phase diagram is less understood. In this region an intermediate antiferromagnetic (AFM) phase appears at higher temperatures up to $\sim$130 K, above which the material becomes paramagnetic (PM). The presence of this AFM phase at low x and intermediate temperatures, displaying AFM coupling between Gd ions across slabs but ferromagnetic (FM) coupling within the slabs,[8] is indicative of the close proximity in total energy between FM and AFM phases in the low-x region of the phase diagram.[9] A contraction of the lattice, either through Si-doping or applied pressure, enhances the interslab interactions and stabilizes FM order. However, the mechanism leading to the emergence of FM-orthorhombic O(I) order from within the AFM-orthorhombic O(II) phase of the Gd_5Ge_4 parent compound at low x is still a matter of debate. In particular, the question arises whether the low-x samples should be described as AFM [O(II)]/FM [O(I)] mixtures or otherwise as structurally homogeneous ternary solid solutions where competing FM and AFM interactions are simultaneously present.[10] Because of the strong electron-lattice coupling present in these compounds, both scenarios are expected to result in an inhomogeneous magnetostructural ground state. This inhomogeneity could in principle be removed by expanding the lattice volume, which favors an AFM phase, or by contracting the lattice with external pressure or chemical pressure (Si doping), which favors the FM state.[11–14]

In this work we present evidence from x-ray diffraction, temperature-dependent bulk magnetization measurements, and x-ray magnetic circular dichroism (XMCD) measurements at ambient- and high-pressure conditions, indicating that the magnetism of low-x samples ($0<x<0.075$) is characterized by the simultaneous presence of the AFM-O(II) and FM-O(I) phases, their volume fractions depending not only on Si content x but also on applied pressure and magnetic field. The application of pressure reduces the lattice volume and stabilizes the FM-O(I) phase, leading to a magnetically and structurally homogeneous ground state, where ordered magnetic moments typical of high-x samples are recovered.

The paper is organized as follows. In Sec. II we describe experimental details, while Sec. III contains the experimental results. The discussion is presented in Sec. IV, and a summary is given in Sec. V.

II. EXPERIMENT

Polycrystalline samples of $Gd_5(Si_xGe_{1-x})_4$ with $x=0$, 0.025, 0.05, 0.075, 0.125, and 0.5 were prepared at Ames Laboratory as detailed in Refs. 14 and 15. The samples were heat treated at 1300 °C for 1 h to achieve homogeneous atomic distribution, and then were finely ground into micron-sized powders. X-ray-diffraction patterns were collected on a Rigaku TTRAX rotating anode powder diffractometer using Mo $K\alpha$ radiation and fitted by Rietveld refinement. The x-ray powder-diffraction measurements at temperatures from 10 to 300 K and in magnetic fields from 0 to 30 kOe were per-

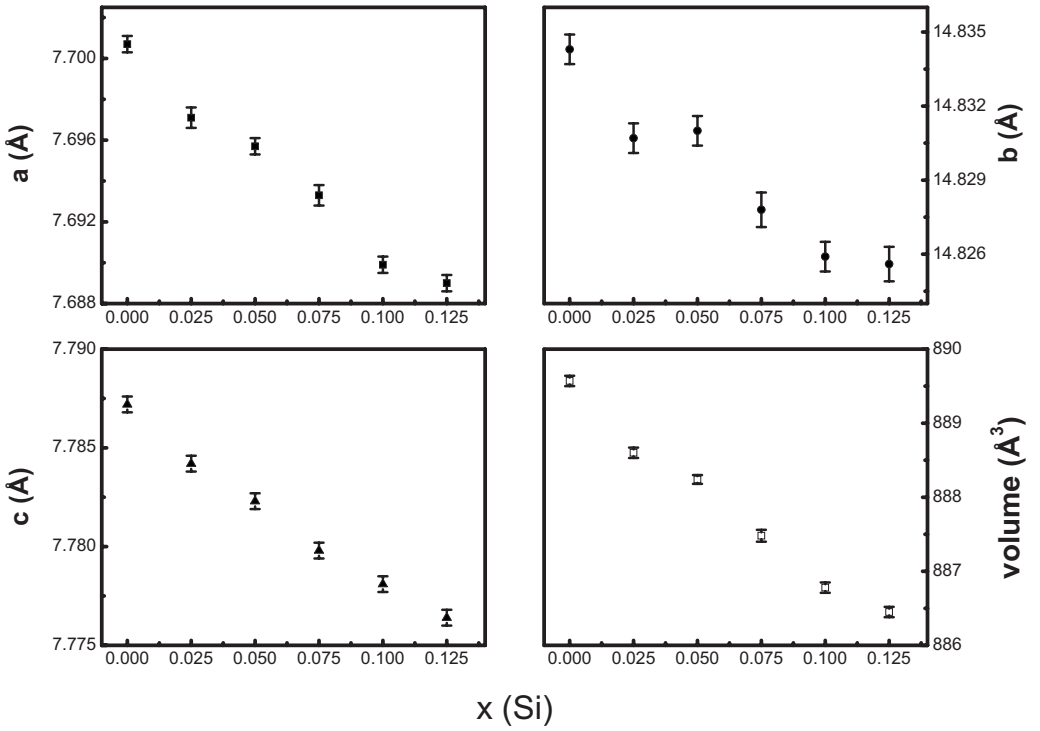

FIG. 1. Lattice parameters and unit-cell volume of $Gd_5(Si_xGe_{1-x})_4$ alloys at room temperature as a function of Si content. All samples exhibit the O(II)-type structure at ambient conditions.

formed on the same diffractometer equipped with a continuous flow helium cryostat and a superconducting magnet.[16] Room-temperature results show a nearly linear dependence of the lattice parameters on Si content, indicating that Si incorporates into the lattice (Fig. 1). Superconducting quantum interference device (SQUID; Quantum Design MPMS XL-7) measurements of the dc magnetic susceptibility in a 50 Oe applied field, both for field cooling (FC) and zero-field cooling (ZFC), show that all samples display ferromagnetic transitions with T_C values of 32, 46, 58, 80, and 275 K for $x=0.025$, 0.05, 0.075, 0.125, and 0.5, respectively (Fig. 2).

In this work only $x=0.025$, 0.05, and 0.075 samples were investigated under high pressure as results on higher-x samples were previously reported.[11] The sample powders were thoroughly mixed with silicon oil which served as pressure medium, with a weight ratio of 1:2. The mixture of sample and medium was loaded into the 250 μm hole of a nonmagnetic stainless-steel gasket which was preindented to 60 μm. A copper-beryllium piston-cylinder diamond-anvil cell (DAC) was used for the low-temperature measurements. Further details on diamond-anvil configuration and implementation of DAC environment for XMCD measurements can be found in Refs. 17 and 18. In the experiments, the ruby fluorescence method[19] was adopted for *in situ* pressure calibration carried out both at 17 and 300 K. To this end, micron-sized ruby powders were added onto the culet face of the minianvil[17,18] before the gasket was loaded. The DAC was mounted on a He-flow cryostat, which is placed between the pole pieces of an electromagnet producing a 7 kOe magnetic field (H) at the sample position. The XMCD measurements were carried out at beamline 4-ID-D of the Advanced Photon Source, Argonne National Laboratory. XMCD was measured at the Gd L_3 edge (7.243 keV), which probes the Gd 5d states at various temperature and pressure conditions. Circularly polarized x rays (Pc$>$95%) were generated using phase-retarding optics.[20,21] XMCD was measured by switching x-ray helicity (12.7 Hz) and detecting the related modulation in absorption coefficient with a lock-in amplifier.[22] All x-ray measurements were done in transmission geometry on warming after ZFC with the magnetic field applied along the x-ray propagation direction.

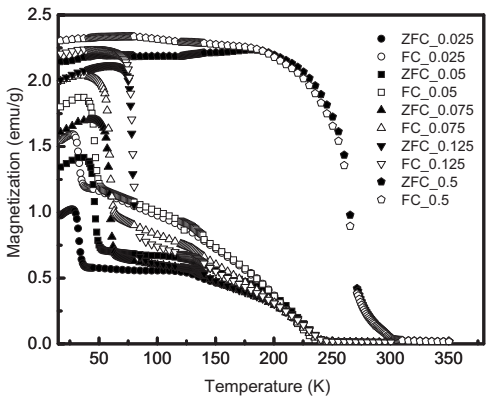

FIG. 2. Temperature-dependent dc magnetization data of $Gd_5(Si_xGe_{1-x})_4$ alloys for $x=0.025$, 0.05, 0.075, 0.125, and 0.5 samples measured on warming in a $H=50$ Oe applied field after field cooling and zero-field cooling.

III. RESULTS

The lattice parameters (a, b, and c) and unit-cell volume as a function of x are plotted in Fig. 1. All samples have a

PM-orthorhombic O(II) phase at room temperature. Figure 2 shows the temperature-dependent FC and ZFC SQUID magnetization data measured on warming for low-x (0.025, 0.05, and 0.075) and higher-x (0.125, and 0.5) samples. According to the Gd_5Si_4-Gd_5Ge_4 phase diagram,[15] the lowest temperature transition found in $x=0.025$, 0.05, 0.075, and 0.125 samples on warming is FM→AFM, and the second transition displaying an anomaly at ~130 K is AFM→PM, which occurs only for $x<0.2$ where an AFM intermediate phase is present.[1–3,9,15,23] The anomalies observed around 230 K in all samples with $x\leq 0.125$ are related to the emergence of the Griffiths phase.[24] The $x=0.5$ sample only shows a FM→PM transition. The FM ordering temperature T_C increases linearly with x as expected.[1,15,23] Most strikingly, the low-temperature magnetization systematically increases with x in both FC and ZFC data for samples with $x<0.125$. Furthermore, significant irreversibility between FC and ZFC data is observed in these low-x samples, whereas this irreversibility is much less significant and almost absent in $x=0.125$ and 0.5 samples.

The x-ray-diffraction pattern measured at ambient pressure and 17 K for the $x=0.025$ sample is shown in Figs. 3(a) and 3(b), together with Rietveld refinements using single phase [O(I)] and mixed-phase [O(I)+O(II)] models. The Rietveld refinements show that both O(II) and O(I) phases are present in this sample, with roughly equal volume fractions at $T=17$ K. The fraction of O(I) phase at low temperature increases with Si doping, reaching 80% for $x=0.05$. It is also observed that the application of a magnetic field (H) increases the volume fraction of the O(I) phase at the expense of the O(II) phase, as shown in Fig. 3(c). A field-induced transition from AFM-O(II) to FM-O(I) was previously reported in single-phase Gd_5Ge_4.[7]

Figure 4 shows representative Gd L_3-edge absorption $(\mu^+ + \mu^-)/2$ and XMCD $(\mu^+ - \mu^-)$ data for the $x=0.025$ sample at 17 K and $P=9.2$ GPa. Here μ^+ and μ^- are x-ray-absorption coefficients for opposite incident x-ray helicity. The inset shows full reversal of XMCD signal upon reversal of a 7 kOe applied field. Since helicity switching is equivalent to magnetization reversal, this is expected and confirms lack of experimental artifacts in the detection system. Data of comparable quality were obtained for all other pressures in this and other samples.

Figure 5 shows the temperature dependence of the integrated XMCD signal measured in a 7 kOe applied field for the three low-x samples at ambient pressure. The integrated signals are proportional to the sample's net magnetization. The data show two clear phase transitions. According to the phase diagram,[14,23] and as seen in Fig. 2, the first transition on warming is an FM→AFM transition while the second transition is AFM→PM, as indicated in the figure. The much more pronounced FM component measured by XMCD above the FM-AFM transition temperature as compared to the SQUID data in Fig. 2 is due to the canting of AFM ordered moments under the $H=7$ kOe applied field.[11] The saturated XMCD values for FM and canted-AFM phases are henceforth labeled as M_s(FM) (for $T<T_C$) and M_s(AFM) (for $T_C<T<T_N$), respectively. These values are proportional to the net FM component in either phase.

Figures 6(a)–6(c) show temperature-dependent XMCD intensities measured at various applied pressures for

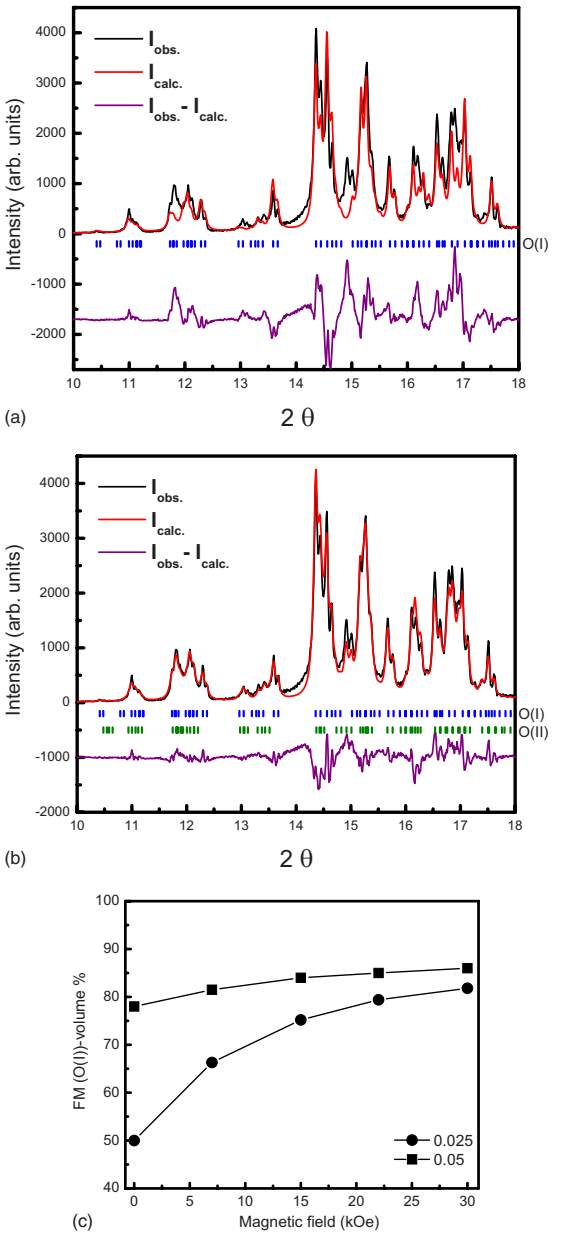

FIG. 3. (Color online) X-ray-diffraction pattern of $Gd_5(Si_xGe_{1-x})_4$ for $x=0.025$ at $H=0$, $T=17$ K together with results of Rietveld refinements using (a) single-phase O(I) structure and (b) mixed-phased O(II)/O(I). Quality of fit parameters is $R_p=22.52\%$, $R_{wp}=28.04\%$, $R_{\mathrm{Bragg}}=16.12\%$ for the single-phase model and $R_p=9.95\%$, $R_{wp}=13.15\%$, $R_{\mathrm{Bragg}}=5.52\%$ for the mixed-phase model. The x-dependent FM-O(I) volume fraction at $T=17$ K is shown in (c) as a function of applied field H. Only small fractions of the pattern are shown in (a) and (b) for clarity.

$x=0.025$, 0.05, and 0.075 samples. It can be seen that pressure initially induces a systematic increase in M_s(FM) and Curie temperature T_C, while M_s(AFM) and associated Néel temperature $T_N\sim 130$ K remain nearly unchanged. At larger pressures, the intermediate AFM phase is no longer present and the data display a single FM→PM transition with a pressure-enhanced T_C.

The pressure dependence of M_s(FM) for the three low-x samples and for $x=0.125$ (the latter taken from Ref. 18) is

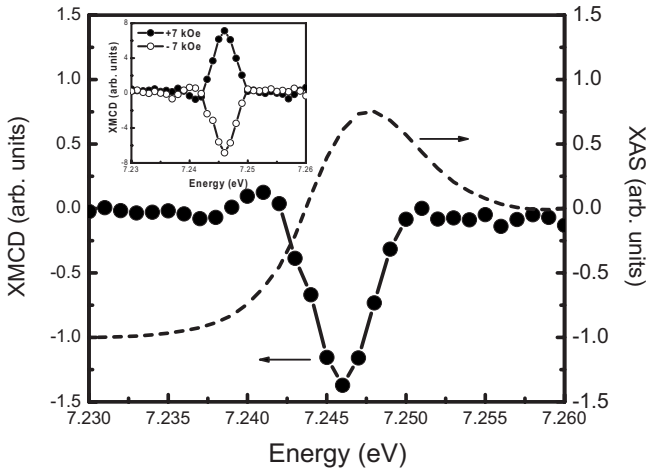

FIG. 4. X-ray absorption (dashed lines) and edge-jump normalized XMCD signal at the Gd L_3 edge of $Gd_5(Si_xGe_{1-x})_4$ alloys for $x=0.025$ at $T=15$ K, $P=9.2$ GPa, and $H=7$ kOe. Inset shows the reversal of XMCD signal upon reversal of the applied magnetic field.

summarized in Fig. 7. All M_s(FM) data are for $T=17$ K and $H=7$ kOe. The pressure dependence of T_C and T_N for the three samples is summarized in Fig. 8. When both FM and AFM transitions are present (low pressure) T_C and T_N are defined as the local maxima in the absolute value of the data's first derivatives for the corresponding transitions. Generally, this corresponds to a ~60% reduction in magnetization relative to M_s(FM,AFM). At higher pressures where a single transition is observed T_C is defined where the XMCD is reduced by ~60% from M_s(FM).

IV. DISCUSSION

The presence of a significant volume fraction of the O(II) phase (50%) for $x=0.025$ [Fig. 3(c)] at $H=0$ kOe and $T=17$ K at ambient pressure is a result of the close proximity in the total energy of FM-O(I) and AFM-O(II) phases at low x. The mixed-phase nature of the sample can be directly associated with the irreversible behavior observed in FC and

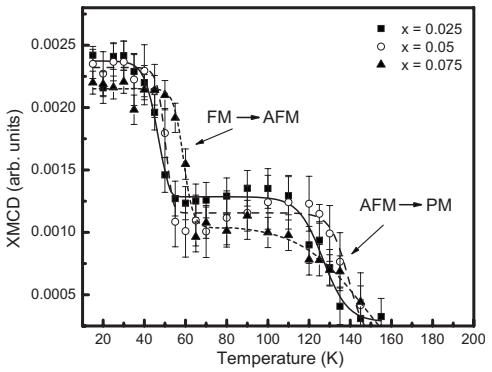

FIG. 5. Temperature-dependent Gd L_3-edge XMCD integrated intensities of $Gd_5(Si_xGe_{1-x})_4$ alloys for $x=0.025$, 0.05, and 0.075 measured at ambient-pressure in $H=7$ kOe. Lines through data point are guides for the eyes.

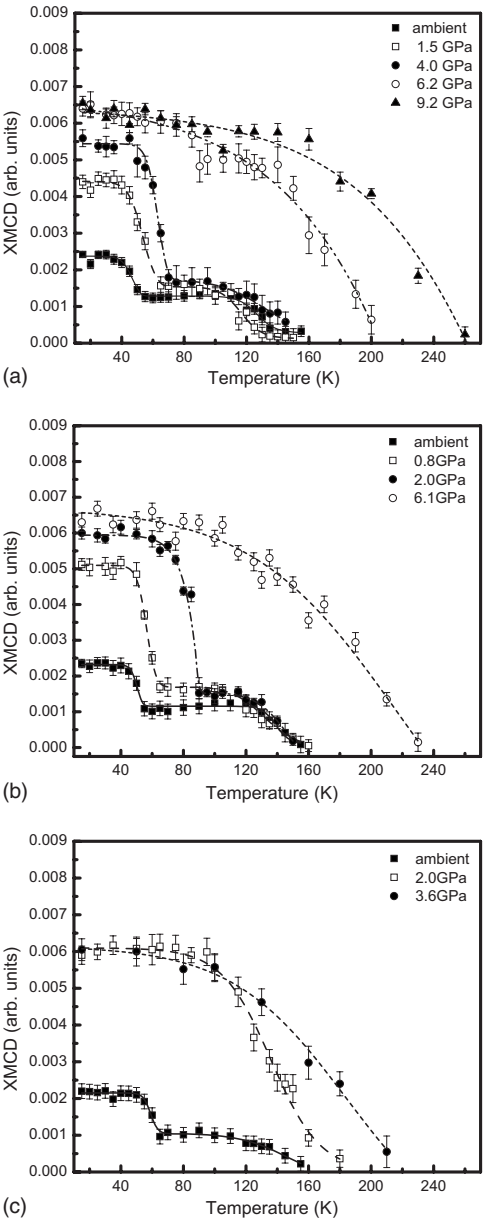

FIG. 6. Temperature dependencies of integrated XMCD intensities of $Gd_5(Si_xGe_{1-x})_4$ alloys for (a) $x=0.025$, (b) $x=0.05$, and (c) $x=0.075$ at various applied pressures.

ZFC SQUID measurements for 0.025, 0.05, and 0.075 samples (Fig. 2) since an applied magnetic field stabilizes the FM-O(I) phase. The larger irreversibility occurs for $x=0.025$, which has the largest AFM fraction. The irreversibility between FC and ZFC magnetization data decreases with increasing x (Fig. 2) as the fractional volume of the AFM-O(II) phase decreases (Fig. 3). This irreversibility is nearly absent in $x=0.125$ and $x=0.5$ samples which show pure Gd_5Si_4-type O(I) phase in the ground state.[5,24] The results show that the presence of the AFM component is responsible for the reduced M_s(FM) seen in $x=0.025$, 0.05, and 0.075 samples. Increasing Si content stabilizes the FM-O(I) phase at the expense of the AFM-O(II) phase, with M_s(FM) reaching saturation at $x\sim0.125$. The low M_s(FM) obtained for the three low-x samples can be thought of as due to composi-

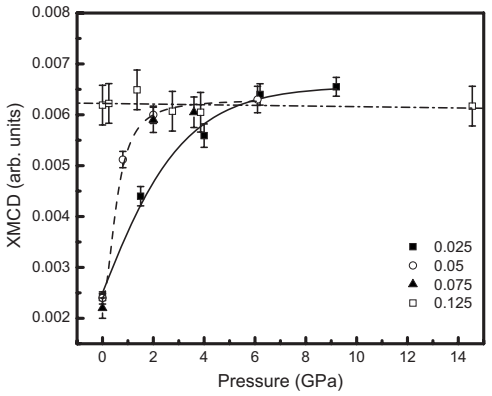

FIG. 7. Saturated magnetization, M_s(FM), as a function of pressure in $Gd_5(Si_xGe_{1-x})_4$ alloys for $x=0.025$, 0.05, 0.075, and 0.125. Data are obtained from integrated XMCD intensities at $T=17$ K.

tional frustration, where FM and AFM components coexist within the sample volume. This behavior is strongly x dependent for $0<x<0.075$ and disappears between $x=0.075$ and $x=0.125$.

The temperature-dependent XMCD intensities depicted in Fig. 5 show that T_C increases with Si doping ($x=0.025, 0.05, 0.075$) at an estimated rate dT_C/dx 4.2 K/Si%. This is in agreement with the 5.0 K/Si% estimated from the phase diagram.[14,23] Additionaly, the $T_N\sim 130$ K found by XMCD is nearly independent of x, also in agreement with previous findings.[14,23] We note that the systematic increase in low-temperature magnetization with increasing x observed in the low-field ($H=50$ Oe) SQUID measurements (Fig. 2) is not evident in the high-field (7 kOe) XMCD measurements. The stronger 7 kOe applied field results in the low-temperature XMCD signal including contributions from both FM-O(I) and *canted* AFM-O(II) phases. These contributions have opposite x dependencies, the FM-O(I) increasing with x and the AFM-O(II) decreasing with x. This compensation

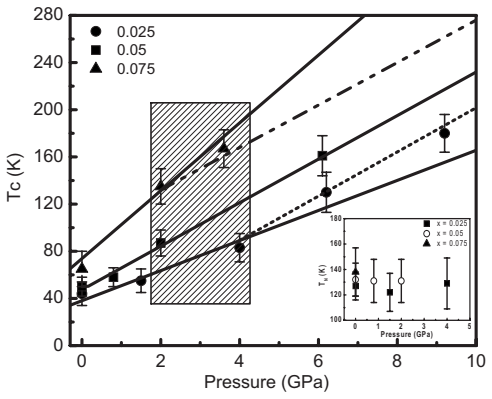

FIG. 8. The pressure dependence of Curie temperature (T_C) and Néel temperature (T_N, inset figure) of $Gd_5(Si_xGe_{1-x})_4$ alloys for $x=0.025$, 0.05, and 0.075 samples. Dashed lines correspond to $dT_C/dP=1.85$ K kbar^{-1}, close to the $dT_C/dP=1.2-1.5$ K kbar^{-1} values found for higher-x 0.125 and 0.375 samples. The shadowed area indicates pressures below (above) which an inhomogeneous (homogeneous) magnetostructural ground state is present at low temperature.

results in a much weaker x dependence of the low-temperature magnetization in the high-field XMCD measurements.

The low-temperature magnetization of the low-x samples at ambient pressure is reduced relatively to the values achieved under high pressure (Figs. 6 and 7). This behavior is different than what we reported previously for $x=0.125$ and 0.5 samples,[11,17] where pressure, much like Si doping, enhances T_C but does not affect the saturation magnetization. Here, pressure increases both T_C and the net FM moment at low temperature. After the saturation magnetization ($H=50$ Oe) reaches values typical of fully ordered FM compounds, such as $x=0.125$ and $x=0.5$, an additional increase in pressure only causes an increase in T_C without further changes in M_s(FM). The different behavior of low-x and high-x samples is due to the presence of an AFM-O(II) phase in the low-x samples. Pressure transforms the AFM phase into the FM phase[25] and M_s(FM) increases accordingly. As shown in Fig. 7, applied pressures of $\sim$5.0, 3.0, and 2.0 GPa are needed to fully convert the low-x inhomogeneous AFM/FM samples [low M_s(FM)] into a homogeneous FM [large M_s(FM)] phase for $x=0.025$, 0.05, and 0.075, respectively.

A pressure-induced AFM→FM transition is known to occur in Gd_5Ge_4, as originally reported by Magen *et al.*[25] It is shown that the AFM-O(II) structure featuring disconnected Gd slabs can be transformed into a FM-O(I) phase at a pressure $P\sim 1$ GPa. Pressure reduces the lattice volume and causes the reforming of Ge-Ge bonds connecting Gd slabs leading to emergence of FM order. Similarly, Pecharsky *et al.*[7] reported that this AFM→FM transition can be induced by magnetic fields where a 93% FM-O(I) volume fraction is observed for $H=3.5$ T. Our field-dependent [Fig. 3(c)] and high-pressure (Fig. 7) results are consistent with these studies, suggesting that the pressure-induced increase in FM interactions within the inhomogeneous AFM/FM ground state (the three low-x samples) is qualitatively similar to what is observed in Gd_5Ge_4. However, in Gd_5Ge_4, the pressure- and field-induced AFM→FM transitions are first order[4,7,25] while field- and pressure-induced transitions in the mixed phase of the low-x samples appear sluggish, requiring significantly larger pressures and fields [Figs. 3(c) and 7]. In what follows we address possible reasons for this behavior.

The AFM→FM transition in $Gd_5(Si_xGe_{1-x})_4$ is coupled to a martensiticlike structural change,[5–7,23] which can occur rapidly under the presence of an effective stress. However, the growth of the martensite phase has to be along the habit plane,[26] which allows the occurrence of macroscopic shape deformation; e.g., in our case, the habit plane is the a axis along which the atomic displacements during the breaking and reforming of Ge-Ge bonds connecting Gd slabs take place.[5–7,23]

However, the growth of the martensite phase together with the concomitant appearance of FM order will be retarded by defect-rich interfacial boundaries as has been reported in surface-related studies.[27] This type of defect-rich boundary is bound to exist in an inhomogeneous AFM[O(II)]/FM[O(I)] phase, which bears large structural misfit, acting as barrier to hinder the growth of the FM-O(I) phase under applied pressure or field, leading to the sluggish

behavior seen in Figs. 3(c) and 7. Obviously, other details of a sample's microstructure will also play a role in determining the dynamics of the phase transition.

Alternatively, the sluggish nature of the pressure- and field-induced transition in the low-x samples could be attributed to the existence of a glasslike state for low applied fields and temperatures rendering the materials into a kinetically arrested state.[28] For example, glasslike dynamics has been observed in Gd_5Ge_4 in the presence of a complex AFM structure.[29] This glassy state varies with T and H and was observed in Gd_5Ge_4 for $H \lesssim 2.5$ T and $T \lesssim 30$ K.[28] Within this H-T region the AFM$\rightarrow$FM transition was found to be sluggish while a sharp first-order transition is recovered away from this H-T boundary. In samples with low Si content, the energy barrier between AFM-O(II) and FM-O(I) states may be lowered, preventing formation of a highly metastable state. In such case a gradual transformation is expected instead of a sharp one. The irreversibility, however, suggests that the kinetic arrest is still present in these samples. The compositional disorder (uneven Si distribution through the lattice), phase coexistence, and complex magnetic structure create a highly frustrated system with multiple energy barriers, which may or may not be easily overcome by external influences.

Thus, it is remarkable that applied pressure restores near full FM-O(I) order at the expense of reducing the fractional volume of the AFM-O(II) phase. The pressure-induced lattice contraction enhances intralayer and interlayer Gd-Gd indirect exchange interactions. Recently, spin-dependent hybridization between Gd $5d$ and Ge $4p$ (Si $3p$) states was reported to change dramatically at the magnetostructural transition affecting the overlap between Gd $5d$ states and the strength of indirect FM exchange.[30] A volume reduction with pressure results in band broadening and a related increase in the overlap between Gd $5d$ states resulting in enhanced long-range indirect Ruderman-Kittel-Kasuya-Yoshida (RKKY) exchange coupling.[11,31] The lower total energy of the FM-O(I) phase versus the AFM-O(II) phase for contracted lattices is the driving force for the pressure-induced and Si-doping (x)-induced transition from an inhomogeneous AFM/FM state into a nearly homogeneous FM state.

Since the AFM-O(II)/FM-O(I) ratio decreases with x (Fig. 3) the pressure needed to achieve a homogeneous FM-O(I) ground state also decreases with x (Fig. 7). We note that, while both M_s(FM) ($T \ll T_C$) and T_C increase with pressure, M_s(AFM) ($T_C < T < T_N$) and T_N are only weakly dependent on pressure [Figs. 6(a)–6(c)]. This is consistent with previous reports on Gd_5Ge_4 (Ref. 25) and $Gd_5Si_{0.125}Ge_{3.875}$,[11] where a much weaker pressure dependence is reported for T_N than for T_C. Pressure increases the fractional volume of the FM state in the mixed ground state ($T \ll T_C$) at the expense of the AFM phase but does not significantly affect the AFM-O(II) structure that is energetically favorable at higher temperature ($T_C < T < T_N$). At small enough volumes (high pressures or $x > 0.2$) the FM-O(I) phase is stabilized to higher T and the AFM-O(II) phase is no longer present.

The ability of pressure and Si doping to restore a homogeneous FM ground state in the low-x samples confirms the previously established concept[11,13] that a unit-cell volume reduction, either through Si doping or applied pressure, enhances the FM exchange interactions and leads to enhanced T_C. However, in a previous pressure study we found $dT_C/dP = 1.2-1.5$ K kbar^{-1} for samples with $x=0.125$ and $x=0.375$ (Refs. 11 and 32); i.e., at these higher doping levels ($0.125 < x < 0.5$) the rate at which T_C increases with pressure is nearly independent of Si concentration provided that applied pressures are small enough that a structural phase transition from monoclinic to orthorhombic-O(I) is not induced at room temperature.[32] We argued that this is due to the fact that the strength of ferromagnetic interactions is mostly determined by lattice volume and hence dT_C/dP is dictated by the lattice compressibility. In contrast, the low-x samples show markedly different behavior. At low pressures $P \lesssim 4$ GPa, dT_C/dP shows strong x dependence, with values of 1.28, 1.85, and 2.87 K kbar^{-1} obtained for $x=0.025$, 0.05, and 0.075, respectively (solid lines in Fig. 8).

This could be interpreted as a result of different compressibilities for these low-x samples associated with the x-dependent fractional volumes of AFM-O(II) and FM-O(I) phases in the mixed state. However, were these samples to have different compressibilities, one would expect the lowest x sample with the largest O(II) fractional volume and largest unit-cell volume to have the largest compressibility and the largest dT_C/dP, while the opposite is observed. [We lack direct measurements of the compressibility of low-x samples at this point to verify this conjecture. However, in $Gd_5Si_2Ge_2$ the large-volume monoclinic phase has greater compressibility than the small-volume O(I) phase.[33]]

On the other hand the martensiticlike, magnetostructural transition AFM-O(II)$\rightarrow$FM-O(I) is expected to be affected by strain. The gradual reduction in interfacial O(II)/O(I) volume in the mixed-phase low-x samples in going from $x=0.025$ to $x=0.075$ may explain the observed changes in dT_C/dP since the sample with largest nominal strain ($x=0.025$) displays the slowest pressure-induced increase in T_C. One would expect that once a homogeneous FM-O(I) state is reached for $P \gtrsim 4$ GPa values of $dT_C/dP \sim 1.2-1.5$ K kbar^{-1} typical of $x=0.125$ and 0.375 samples would be restored.[32] Although the limited number of data points in Fig. 8 precludes us from making a definitive statement, the available data are consistent with this expectation (dashed lines in Fig. 8 correspond to $dT_C/dP = 1.85$ K kbar^{-1}).

We end the discussion by comparing dT_C/dP in Gd_5Ge_4, low-x samples ($x=0.025$, 0.05, and 0.075), and high-x samples ($x=0.125, 0.375$). The largest dT_C/dP of ~ 4.8 K kbar^{-1} is obtained for Gd_5Ge_4, followed by the low-x samples (1.28, 1.85, and 2.87 K kbar^{-1} for $x=0.025$, 0.05, and 0.075, respectively) while the smallest dT_C/dP of 1.2–1.5 K kbar^{-1} is obtained for $x=0.125$ and $x=0.375$. In Gd_5Ge_4, the pressure-induced first-order transition from AFM-O(II) to FM-O(I) involving the reforming of Ge-Ge bonds connecting Gd slabs leads to a sudden stabilization of the FM state. For the mixed-phase low-x samples discussed here, the ability of applied pressure to stabilize a homogeneous FM state is strongly dependent on the level of Si doping, i.e., on the AFM-O(II)/FM-O(I) ratio. When the FM-O(I) phase is fully developed for $x=0.125$ and 0.375 samples (or for $P \gtrsim 4$ GPa in low-x samples), pressure enhances FM ordering at the slowest rate. The drastic change in dT_C/dP

behavior, which increases in low-x samples from 0.025 to 0.075 but decreases to become constant in higher-x samples ($0.1 < x < 0.5$) (Ref. 32) and in low-x samples at high pressures is further evidence that the exchange interactions in the low-x region of the phase diagram are influenced by Si doping in a way that is fundamentally different than what takes place in the high-x region of the phase diagram.

V. SUMMARY

The magnetic and structural properties of low-x (0.025, 0.05, and 0.075) Ge-rich $Gd_5(Si_xGe_{1-x})_4$ compounds were probed with element-specific XMCD measurements in a diamond-anvil cell, together with SQUID magnetometry and x-ray-diffraction measurements. While the small Si-doping levels lead to emergence of partial FM order, the ground state is inhomogeneous due to an incomplete AFM→FM transition on cooling. This inhomogeneous ground state features a reduced low-temperature magnetization accompanied by strong irreversibility in FC and ZFC magnetization data, indicative of glassy behavior. Applied pressure reduces the lattice volume and enhances the FM exchange interactions, restoring a nearly fully ordered FM state. Although T_C increases with pressure as previously observed in high-x samples,[11,13] dT_C/dP is strongly x dependent for low-x samples in contrast with the nearly x-independent dT_C/dP found for $0.125 < x < 0.5$.[32] The results suggest that the emergence of FM from within the AFM phase of Gd_5Ge_4 cannot simply be described by a volume effect and that the presence of an inhomogeneous magnetostructural ground state ought to be considered in order to explain the rather complex low-x region of the phase diagram of these materials.

ACKNOWLEDGMENTS

The work at Argonne and Ames was supported by the U.S. Department of Energy, Office of Science and Office of Basic Energy Sciences, under Contracts No. DE-AC-02-06CH11357 and No. DE-AC02-07CH1358, respectively.

*haskel@aps.anl.gov

[1] V. K. Pecharsky and K. A. Gschneidner, Phys. Rev. Lett. **78**, 4494 (1997).
[2] A. Giguére, M. Foldeaki, B. Ravi Gopal, R. Chahine, T. K. Bose, A. Frydman, and J. A. Barclay, Phys. Rev. Lett. **83**, 2262 (1999).
[3] J. R. Sun, F. X. Hu, and B. G. Shen, Phys. Rev. Lett. **85**, 4191 (2000).
[4] L. Morellon, P. A. Algarabel, M. R. Ibarra, J. Blasco, B. Garcia-Landa, Z. Arnold, and F. Albertini, Phys. Rev. B **58**, R14721 (1998).
[5] W. Choe, V. K. Pecharsky, A. O. Pecharsky, K. A. Gschneidner, Jr., V. G. Young, Jr., and G. J. Miller, Phys. Rev. Lett. **84**, 4617 (2000).
[6] V. K. Pecharsky and K. A. Gschneidner, Jr., Adv. Mater. (Weinheim, Ger.) **13**, 683 (2001).
[7] V. K. Pecharsky, A. P. Holm, K. A. Gschneidner, Jr., and R. Rink, Phys. Rev. Lett. **91**, 197204 (2003).
[8] L. Tan, A. Kreyssig, J. W. Kim, A. I. Goldman, R. J. McQueeney, D. Wermeille, B. Sieve, T. A. Lograsso, D. L. Schlagel, S. L. Budko, V. K. Pecharsky, and K. A. Gschneidner, Phys. Rev. B **71**, 214408 (2005).
[9] D. Paudyal, V. K. Pecharsky, K. A. Gschneidner, Jr., and B. N. Harmon, Phys. Rev. B **75**, 094427 (2007).
[10] F. Casanova, S. d. Brion, A. Labarta, and X. Batlle, J. Phys. D: Appl. Phys. **38**, 3343 (2005).
[11] Y. C. Tseng, D. Haskel, J. C. Lang, S. Sinogeikin, Y. Mudryk, V. K. Pecharsky, and K. A. Gschneidner, Phys. Rev. B **76**, 014411 (2007).
[12] A. M. G. Carvalho, Cleber S. Alves, Ariana de Campos, Adelino A. Coelho, Sergio Gama, Flavio C. G. Gandra, Pedro J. von Ranke, and Nilson A. Oliveira, J. Appl. Phys. **97**, 10M320 (2005).
[13] L. Morellon, Z. Arnold, P. A. Algarabel, C. Magen, M. R. Ibarra, and Y. Skorokhod, J. Phys.: Condens. Matter **16**, 1623 (2004).
[14] V. K. Pecharsky and K. A. Gschneidner, Jr., Appl. Phys. Lett. **70**, 3299 (1997).
[15] V. K. Pecharsky and K. A. Gschneidner, Jr., J. Alloys Compd. **260**, 98 (1997).
[16] A. P. Holm, V. K. Pecharsky, K. A. Gschneidner, Jr., R. Rink, and M. Jirumanus, Rev. Sci. Instrum. **75**, 1081 (2004).
[17] D. Haskel, Y. C. Tseng, J. C. Lang, and S. Sinogeikin, Rev. Sci. Instrum. **78**, 083904 (2007).
[18] D. Haskel, Y. C. Tseng, N. M. Suoza-Neto, J. Lang, S. Sinogeikin, Y. Mudryk, V. K. Pecharsky, and K. A. Gschneidner, Jr., High Press. Res. **28**, 185 (2008).
[19] K. Syassen, High Press. Res. **28**, 75 (2008).
[20] K. Hirano, K. Izumi, T. Ishikawa, S. Annaka, and S. Kikuta, Jpn. J. Appl. Phys., Part 2 **30**, L407 (1991).
[21] J. C. Lang and George Srajer, Rev. Sci. Instrum. **66**, 1540 (1995).
[22] M. Suzuki, N. Kawamura, M. Mizumaki, A. Urta, H. Maruyama, S. Goto, and T. Ishikawa, Jpn. J. Appl. Phys., Part 2 **37**, L1488 (1998).
[23] L. Morellon, J. Blasco, P. A. Algarabel, and M. R. Ibarra, Phys. Rev. B **62**, 1022 (2000).
[24] Ya. Mudryk, D. Paudyal, V. K. Pecharsky, and K. A. Gschneidner, Jr., Phys. Rev. B **77**, 024408 (2008).
[25] C. Magen, Z. Arnold, L. Morellon, Y. Skorokhod, P. A. Algarabel, M. R. Ibarra, and J. Kamarad, Phys. Rev. Lett. **91**, 207202 (2003).
[26] *Martensite*, edited by G. B. Olson and W. S. Owen (ASM International, Materials Park, Ohio, 1992), Chaps. 7, 9, and 10.
[27] P. Pörsch, M. Kallmayer, T. Eichhorn, G. Jakob, H. J. Elmers, C. A. Jenkins, C. Felser, R. Ramesh, and M. Huth, Appl. Phys. Lett. **93**, 022501 (2008).
[28] V. K. Pecharsky and K. A. Gschneidner, Jr., Pure Appl. Chem. **79**, 1383 (2007).
[29] S. B. Roy, M. K. Chattopadhyay, P. Chaddah, J. D. Moore, G. K. Perkins, L. F. Cohen, K. A. Gschneidner, and V. K. Pecharsky,

Phys. Rev. B **74**, 012403 (2006).
[30] D. Haskel, Y. B. Lee, B. N. Harmon, Z. Islam, J. C. Lang, G. Srajer, Ya. Mudryk, K. A. Gschneidner, Jr., and V. K. Pecharsky, Phys. Rev. Lett. **98**, 247205 (2007).
[31] M. A. Ruderman and C. Kittel, Phys. Rev. **96**, 99 (1954); T. Kasuya, Prog. Theor. Phys. **16**, 45 (1956); K. Yosida, Phys. Rev. **106**, 893 (1957).
[32] Y. C. Tseng, D. Haskel, J. Lang, Y. Mudryk, V. K. Pecharsky, and K. A. Gschneidner, Jr., J. Appl. Phys. **103**, 07B301 (2008).
[33] Ya. Mudryk, Y. Lee, T. Vogt, K. A. Gschneidner, Jr., and V. K. Pecharsky, Phys. Rev. B **71**, 174104 (2005).